Coherent Optical MIMO (COMIMO)

Akhil R. Shah, Rick C. J. Hsu, Alireza Tarighat, *Student Member, IEEE*, Ali H. Sayed, *Fellow, IEEE*,
and Bahram Jalali, *Fellow, IEEE*

Abstract—We present a multiple-input multiple-output (MIMO) optical link based on coherent optics and its ability to exploit the inherent information capacity of multimode fiber. A coherent implementation differs from previous work in optical MIMO by allowing the system to tolerate smaller modal delay spreads, because of a much larger carrier frequency, and yet maintain the necessary diversity needed for MIMO operation. Furthermore, we demonstrate the use of MIMO adaptive equalization to mitigate intersymbol interference when exceeding the bandwidth–length product of the link. The impact of phase noise is studied with numerical simulation.

Index Terms—Coherent optics, MIMO, multimode fiber.

I. INTRODUCTION

WIRELESS communication with multiple transmit and receive antennas, referred to as multiple-input multiple-output (MIMO), has garnered significant research interest and prompted commercialization of a relatively new technology that promises to supply the growing demand for link capacity. By exploiting the multipath nature of wireless channels, a trait that inhibits traditional wireless systems, capacity (bits/second/Hertz) can *increase linearly* with the number of transmit and receive antennas [1], while still maintaining the same total transmitted power as a traditional single-transmit/receive antenna system. This remarkable technique implies that at a given receiver signal-to-noise ratio (SNR), total transmit power, and signal bandwidth, one can increase the aggregate data rate linearly by simply adding more antennas.

The linear increase in channel capacity as a function of the number of transmitters/receivers (Tx/Rx), the celebrated result of MIMO communication, has positive consequences for the bandwidth–length (BL) product of optical fiber communications. In ordinary single-input single-output (SISO) fiber communication, for a desired error rate and a given length of fiber, one is limited by dispersion to a maximum data rate or bandwidth that is characterized by the BL product. By comparison, MIMO fiber communication with n lasers and photoreceivers, using the same length of fiber and total transmitted optical power (i.e., each of the n lasers transmits $1/n$ of the optical power transmitted by the laser in the SISO case) one can, by utilizing the MIMO signal processing, increase the channel capacity or equivalently the bandwidth by a factor of n and hence scale the bandwidth as $B_{\text{MIMO}} = nB_{\text{SISO}}$. Alternatively, for the same data rate, one can increase

the length of the link by a factor of n, $L_{\text{MIMO}} = nL_{\text{SISO}}$. Consequently, MIMO signal processing increases the BL by a scale factor equal to the number of Tx/Rx pairs, $\text{BL}_{\text{MIMO}} = n\text{BL}_{\text{SISO}}$.

Of course, this benefit is not without a price, namely, greater complexity in the signal-processing domain. Yet with efficient digital signal processing (DSP) algorithms and hardware implementations, this tradeoff is manageable and certainly worth the effort.

The paper is organized as follows. In the remainder of Section I, we discuss the motivation and traditional approaches for using and improving multimode fiber communication, and second, detail the advantages of the coherent optical MIMO (COMIMO) system. In Section II, we review the MIMO channel model, relate it to the multimode fiber (MMF) physical layer, and briefly discuss relevant signal processing algorithms. In Section III, we detail the implementation of COMIMO. This section also reports the first-ever use of MIMO equalization to mitigate intersymbol interference (ISI) in an optical MIMO system and addresses the impact on MIMO performance due to laser phase noise, topics that have *not* been covered in previous COMIMO literature, [15], [16]. Section IV concludes the paper with a summary of our results and discussion.

A. The Multimode Fiber

MMF has practical advantages over single-mode fiber (SMF) such as increased alignment tolerances and ease of packaging, which can lead to significant cost savings. The main drawback of MMF is the multimode nature of the fiber that gives rise to modal dispersion and limits its bandwidth to a fraction of what can be achieved with SMF. Though it seems that little can be done about the inherent modal dispersion associated with the multimode nature of fibers, researchers have achieved improvements in the bandwidth–distance product of MMF using several approaches such as selective modal excitation [2], [3], m-ary coding [4], electronic equalization [5], [6], and subcarrier multiplexing [7]–[11]. While each of these techniques has shown substantial increases in the bandwidth–distance product, they still do not exploit the MMF capacity to its full potential.

Wavelength-division multiplexing based on MMF links is also a promising way of pushing the limit of overall transmission capacity [12], [13]. However, the cost associated with multiwavelength systems is, so far, still too high to be extensively implemented for commercial use.

B. Advantages of COMIMO

Optical MIMO is based on the analogy between multipath fading in wireless channels and modal dispersion in MMF and
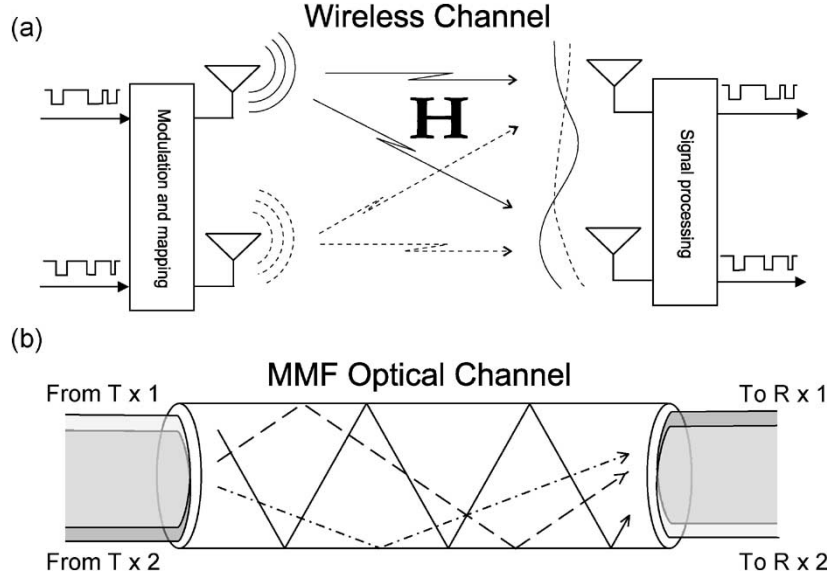
Fig. 1. (a) Coupling diversity into and out of MMF. (b) Ray tracing conceptual description of light beam scattering inside a multimode fiber.

allows transmission of multiple data channels simultaneously through a single fiber. A high-level sketch of the multiple transmitter and receiver system is shown in Fig. 1, along with a ray-tracing representation of scattering in MMF.

Although techniques like selective modal launching also attempt to spatially multiplex data with multiple transmitters and receivers, they avoid modal dispersion, whereas a true MIMO system exploits it. Furthermore, selective modal launching requires a time-invariant channel, for which one must also have an accurate channel model *a priori*. Another distinguishing feature is that MIMO signal processing requires detection of both amplitude and *phase* information, in contrast to pure intensity detection used in conventional fiber-optic links.

Stuart [14] noticed the analogy between wireless and optical channels and demonstrated the feasibility of MIMO over MMF in a two-Tx, two-Rx (2×2) channel experiment. In [14], radio frequency (RF) subcarrier (~ 1 GHz) *intensity modulation* with phase-shift keying (PSK) data format was used at the transmitters followed by recovery of in-phase (I) and quadrature (Q) RF components through synchronous RF demodulation at the receivers. As will be shown in this paper, the use of RF subcarrier intensity modulation and detection requires a very long MMF and places a minimum on the subcarrier frequency in order to ensure enough modal diversity, which is a requirement for MIMO operation.

In contrast, if coherent optical transmission is used, the required length is reduced by the ratio of the RF subcarrier frequency to the optical carrier frequency [15], [16]. This eliminates the length requirement. Similarly, for a given length of fiber, the diversity requirement imposes a low-frequency limit on the subcarrier frequency. For example, using 300 m of 62.5-μm MMF, the diversity requirement is only satisfied for frequencies greater than ~ 3 GHz. This necessitates upconversion of baseband digital data. On the other hand, using coherent optical communication, the baseband data are already upconverted to the optical carrier frequency (hundreds of terahertz), entirely satisfying the diversity requirement [15], [16].

The tremendous advantages afforded by COMIMO for MMF communication are possible through advanced DSP. The use of DSP to enhance the performance of communication links is well established. For example, the emerging IEEE 802.3 10-Gb/s Ethernet standard, which includes MMF as one of the physical-layer options (copper cabling is another medium but is limited to 15 m in length, whereas MMF has a maximum link length of 300 m), is considering electronic dispersion compensation, which is proven to improve link performance [17]. Furthermore, very large scale integration implementations of signal processing algorithms benefit from Moore's law and represent a cost-effective solution.

II. THEORY OF MIMO COMMUNICATION

A simple linear model for a time-invariant SISO flat-communication link is $y_{\text{bp}}(t) = h_0 e^{j\omega_c t} s(t - \tau_g) + v_{\text{bp}}(t)$, where $s(t)$ is transmitted data modulated on a carrier of frequency ω_c, and $y_{\text{bp}}(t)$ is the bandpass data received after a group-delay of τ_g and after being corrupted by multiplicative distortion or *fading* h_0 (usually a complex number) and additive noise v_{bp}. In this example, the channel impulse response $h(t) = h_0 \delta(t - \tau)$ is appropriate for *narrow-band* communication. The following model is often used to represent time-invariant channels that cause ISI as in *wide-band* communication:

$$y_{\text{bp}}(t) = \sum_{k=1}^{P} |h_k| e^{j\omega_c \tau_{\text{p}k}} e^{j\omega_c t} s(t - \tau_{gk}) + v_{\text{bp}}(t) \quad (1)$$

where y_{bp} and v_{bp} are the bandpass received signal and additive noise, respectively; s is the data modulated onto a carrier with frequency ω_c; P is the number of paths in the channel model, $|h_k|$ is the path attenuation, and $\tau_{\text{p}k}$ and τ_{gk} are, respectively, the phase and group-delays associated with that path. As is commonly done in communication theory, we will use a baseband model that assumes perfect homodyne

downconversion of the received bandpass signal to give the received baseband signal $y(t) = e^{-j\omega_c t} y_{\mathrm{bp}}(t)$. It is also common to define the path fading parameter $h_k = |h_k| e^{j\omega_c \tau_{pk}}$.

For simplicity, assume that the sum in (1) is written in order of ascending delay, then the phase-delay spread $\tau_{\mathrm{pd}} = \tau_{pQ} - \tau_{p1}$ and the group-delay spread is $\tau_{\mathrm{gd}} = \tau_{gQ} - \tau_{g1}$. An important point to remember, and which will be explained shortly, is that the larger the product of phase-delay spread and carrier frequency, the greater the spatial diversity in the channel [1]. When $\omega_c \tau_{\mathrm{pd}} \gg 2\pi$, the phase of h_k can be considered a random variable uniformly distributed over $[0, 2\pi)$. An advantage of COMIMO is that ω_c is the optical carrier frequency which is orders of magnitude larger than in an RF subcarrier system and can thus tolerate a smaller phase-delay spread while maintaining spatial diversity [15], [16]. The product of group-delay spread and modulation frequency or data rate will determine whether the channel will induce ISI. When the group-delay spread is small compared to the time scale (i.e., symbol period) of the modulation envelope, as in narrow-band communication, all paths arrive at approximately the same time, i.e., $s(t - \tau_{gk}) \approx s(t - \tau_g)$ for all τ_{gk}. The model of (1) then simplifies to the narrow-band model $y(t) = hs(t - \tau_g) + v(t)$, where the complex scalar $h = \sum_{k=1}^{P} |h_k| e^{j\omega_c \tau_{pk}}$ represents *frequency flat* fading.

If $\omega_c \tau_{pk} \gg 2\pi$, it is assumed that $\angle h$ is a random variable uniformly distributed over $[0, 2\pi)$. Another assumption often made is that the number of paths P is large and by the central-limit theorem and the previous assumption, h is a zero-mean complex random number, which further implies that $|h|$ is a Rayleigh-distributed random variable. The narrow-band model described above is then termed Rayleigh flat fading. Rayleigh fading is often considered a worst case scenario in traditional SISO systems but ironically becomes an optimistic, best case scenario for MIMO [19]. It is critical then to maintain both of the above assumptions and is more feasible when the carrier frequency is larger as in COMIMO, which uses an optical carrier rather than an RF subcarrier to generate channel diversity. The wide-band model $y(t) = \sum_{k=1}^{P} h_k s(t - \tau_{gk}) + v(t)$ with the same assumptions for each path h_k, in addition to the constraint that each path is independent of another [i.e., the h_k are independent identically distributed (i.i.d) zero-mean complex Gaussian], will be referred to as Rayleigh dispersive fading.

A. MIMO Model for the MMF Optical Channel

Each of the above parameters and concepts can be related to the characteristics of MMF. In (1), $h_k = a_k \kappa_k e^{j\omega_c \tau_{pk}}$ where a_k and τ_{pk} represent the attenuation and phase-delay of the kth mode and κ_k represents the fractional power coupled into that mode. Assuming that the loss associated with each mode is the same, the distinguishing characteristic of each mode is its propagation velocity β_k, which relates to the propagation delay as $\tau_{pk} = L/\beta_k$, and thus to the phase-delay spread as $\tau_d = L(1/\beta_Q - 1/\beta_1)$, for a fiber length L.

To extend the above concepts to the case of optical MIMO, assume a link with two Txs and two Rxs. Let $\{x_1(t), x_2(t)\}$ be the data transmitted from Txs 1 and 2, and $\{y_1(t), y_2(t)\}$ be the corresponding received data. For simplicity, we will use

the narrow-band model of Rayleigh flat fading. For each pair of Tx and Rx, we will have a narrow-band channel such that $y_i(t) = h_{ij} s_j(t - \tau_g) + v_i(t)$, where τ_g is the overall latency assumed the same for all paths, and $h_{ij} = \sum_{k=1}^{P} \kappa_k^{(ij)} e^{j\omega_c \tau_{pk}}$. In the Rayleigh flat-fading model, each h_{ij} is a random complex number with amplitude from a Rayleigh distribution and phase from a uniform distribution. Again, assuming linearity, this model can be written succinctly as

$$\begin{pmatrix} y_1(t) \\ y_2(t) \end{pmatrix} = \begin{pmatrix} h_{11} & h_{12} \\ h_{21} & h_{22} \end{pmatrix} \begin{pmatrix} s_1(t - \tau_g) \\ s_2(t - \tau_g) \end{pmatrix} + \begin{pmatrix} v_1(t) \\ v_2(t) \end{pmatrix}. \quad (2)$$

The above matrix equation is noted symbolically as

$$y = \mathbf{H}s + v. \quad (3)$$

To reap the benefits of MIMO, such as linear capacity growth with number of Tx/Rx elements, one must ensure that the matrix elements of H are sufficiently uncorrelated [1] and, in the best case, are i.i.d complex Gaussian random variables (i.e., Rayleigh fading) [19]. To ensure this condition, one needs both: 1) a large product of phase-delay spread and carrier frequency $\omega_c \tau_{\mathrm{pd}} \gg 2\pi$, so the phase of each element of H can be considered a uniformly distributed random variable over $[0, 2\pi)$; and 2) a large number of modes/paths, so that each Tx and Rx launch into and sample from sufficiently different groups of modes/paths. COMIMO eases the restriction on minimum phase-delay spread by using a very large carrier frequency, namely the optical carrier frequency, as explained before.

B. Signal Processing Algorithms

In this section, we will outline signal processing algorithms that allow us to recover data transmitted from multiple Txs and received by multiple Rxs. Unlike other spatial multiplexing techniques, such as selective-mode launching, we do not need to know the channel *a priori* and in fact can estimate the channel with the algorithms below. Furthermore, some algorithms do not even require an estimate of the channel and can recover data directly. As the signal processing is done in the digital domain, we will replace the time dependence of all variables with the nth sampling instant.

Since the h_{ij} are complex, the received data y_i will also be complex, requiring coherent demodulation to recover the transmitted data. The subsequent signal processing can be readily implemented in the electronic domain. Some algorithms require estimation of the channel matrix elements through the use of "training" symbols known at both Tx and Rx. The number of training symbols is usually determined by experimentation, from which the h_{ij} can be computed using least-squares (LS) or recursive algorithms found in adaptive filtering such as least-mean squares (LMS) or recursive least squares (RLS) [20]. Once the channel estimate is obtained from training symbols, the next task of symbol recovery (recovery of nontraining or actual data) can proceed using a variety of algorithms from simply computing the inverse of the matrix and multiplying the incoming received data or using the well-known Vertical Bell Labs Layered Space–Time (V-BLAST) algorithm [21]. MIMO

equalization can offer an alternative scheme whereby training data are used to directly estimate the inverse of the channel matrix, therefore bypassing the need to perform computationally expensive matrix inversion [22].

Channel estimation can be performed by posing a problem similar to (3), except the unknowns are now the channel matrix elements. Consider the following reorganization of the system model equation as $y = \tilde{\mathbf{S}}h + v$ for an N (Rxs) by M (Txs) system, where y is the received matrix of data due to the transmission of l *known* training symbols represented by $\tilde{\mathbf{S}}$ and corrupted by noise v.

$$
\begin{pmatrix} y_1(1) \\ y_1(2) \\ \vdots \\ y_1(l) \\ \vdots \\ y_N(l) \end{pmatrix} = \underbrace{\begin{pmatrix} \tilde{\mathbf{S}} & \mathbf{0} & \dots & \mathbf{0} \\ \mathbf{0} & \tilde{\mathbf{s}} & \dots & \mathbf{0} \\ \vdots & \vdots & \ddots & \vdots \\ \mathbf{0} & \mathbf{0} & \dots & \tilde{\mathbf{s}} \end{pmatrix}}_{\tilde{\mathbf{S}}} \begin{pmatrix} h_{11} \\ h_{12} \\ \vdots \\ h_{1M} \\ \vdots \\ \vdots \\ h_{NM} \end{pmatrix} + v \quad (4)
$$

where each $\tilde{\mathbf{s}}$ is the following matrix

$$
\tilde{\mathbf{s}} = \begin{pmatrix} s_1(1) & \dots & s_M(1) \\ s_1(2) & \dots & s_M(2) \\ \vdots & \vdots & \vdots \\ \vdots & \vdots & \vdots \\ s_1(l) & \dots & s_M(l) \end{pmatrix}
$$

and $\mathbf{0}$ is the $l \times M$ zero matrix. In other words, $\tilde{\mathbf{S}}$ is a block diagonal matrix of *block size* $N \times N$ where each nonzero block is the $l \times M$ matrix $\tilde{\mathbf{s}}$ that represents the training symbols. Note that the *element size* of the matrix $\tilde{\mathbf{S}}$ is thus $lN \times MN$.

Equation (4) is an overdetermined system of linear equations that has an infinite number of solutions for h. One of the most useful solutions is the LS solution, which we shall denote by $\hat{h}$. The LS estimate of the channel $\hat{h}$ has the property that minimizes the error between the actual received versions of the training symbols y and those computed with $\hat{h}$, i.e.,

$$
\|y - \tilde{\mathbf{S}}\hat{h}\| \le \|y - \tilde{\mathbf{S}}\bar{h}\| \quad (5)
$$

where $\bar{h}$ is any other solution of (4).

In the case where $\tilde{\mathbf{S}}$ is *not* rank deficient, it can be shown that [20]

$$
\hat{h} = (\tilde{\mathbf{S}}^*\tilde{\mathbf{S}})^{-1}\tilde{\mathbf{S}}^*y \quad (6)
$$

where $\tilde{\mathbf{S}}^*$ is the complex conjugate transpose of $\tilde{\mathbf{S}}$. If $\tilde{\mathbf{S}}$ is rank deficient, then the LS solution is not unique, and moreover $\tilde{\mathbf{S}}^*\tilde{\mathbf{S}}$ is singular (i.e., noninvertible).

Now assume that $\mathbf{H}$ is a square matrix, i.e., assume the case of equal number of Tx and Rx elements or $M = N$. One way to recover the symbols is to multiply y in (3) by $\mathbf{H}^{-1}$. Denoting the estimated symbol as $\hat{s}$, we see that

$$
\hat{s} = s + \mathbf{H}^{-1}v. \quad (7)
$$

This method is called *zero forcing* (ZF) and has the disadvantage that if the elements of $\mathbf{H}$ are small, then the elements of $\mathbf{H}^{-1}$ will be large and can "amplify" the noise component v and degrade the SNR of the estimated symbol $\hat{s}$, thereby causing an erroneous decision at the receiver. Furthermore, there is the possibility that $M \ne N$ and hence the inverse of $\mathbf{H}$ does not even exist (recall that the matrix inverse is only defined for nonsingular square matrices). One could of course use a *pseudoinverse* of $\mathbf{H}$, but the problem of degraded SNR still remains. The method of [21] is actually an iterative process of determining a pseudoinverse that is mindful of the SNR degradation property of the ZF technique.

Equalization does not require channel estimation and attempts to directly estimate an "inverse" channel that minimizes some error criterion. Although it can be used in the narrowband case as an alternative to channel estimation followed by ZF or V-BLAST symbol recovery, it is more useful in the wideband case, where ISI is significant. As an illustration, a simple wide-band MIMO model for two Txs and Rxs with a maximum of P multipaths between each Tx and Rx can be written succinctly as

$$
\begin{pmatrix} y_1 \\ y_2 \end{pmatrix} = \sum_{k=1}^{P} \begin{pmatrix} h_{11k} & h_{12k} \\ h_{21k} & h_{22k} \end{pmatrix} \begin{pmatrix} s_1(t - \tau_{gk}) \\ s_2(t - \tau_{gk}) \end{pmatrix} + \begin{pmatrix} v_1 \\ v_2 \end{pmatrix} \quad (8)
$$

or in vector–matrix form as $y(t) = \sum_{k=1}^{P} \mathbf{H}_k s(t - \tau_{gk}) + v(t)$.

Such a system can suffer from ISI and requires MIMO equalization. The structure of the equalizer is shown in [22], and the coefficients or tap weights of the equalizer can be determined in a manner similar to the channel estimation problem of (4). The maximum number of equalizer taps needed will depend on the modal energy distribution and group-delay spread which are not known *a priori*. In practice, the number of taps needs to be determined by experimentation to achieve tolerable ISI and error rate. The equalizer tap weights w are determined by again using training symbols (known transmitted data) and solving an analogous least-squares problem $x = \tilde{\mathbf{S}}w + v$, where $\tilde{\mathbf{S}}$ is a matrix of received training symbols defined below. Assuming that the maximum number of taps for an equalizer is Q (not to be confused with P, the maximum number of multipaths; a larger number), and using l training symbols, the matrix equation can be written explicitly as

$$
\begin{pmatrix} x_1(1) \\ x_1(2) \\ \vdots \\ x_1(l) \\ \vdots \\ x_N(l) \end{pmatrix} = \underbrace{\begin{pmatrix} \tilde{\mathbf{s}} & \mathbf{0} & \dots & \mathbf{0} \\ \mathbf{0} & \tilde{\mathbf{s}} & \dots & \mathbf{0} \\ \vdots & \vdots & \ddots & \vdots \\ \mathbf{0} & \mathbf{0} & \dots & \tilde{\mathbf{s}} \end{pmatrix}}_{\tilde{\mathbf{s}}} \begin{pmatrix} w_{11}(1) \\ w_{12}(1) \\ \vdots \\ w_{1M}(1) \\ \vdots \\ w_{11}(Q) \\ \vdots \\ w_{1M}(Q) \\ \vdots \\ w_{MN}(Q) \end{pmatrix} + v \quad (9)
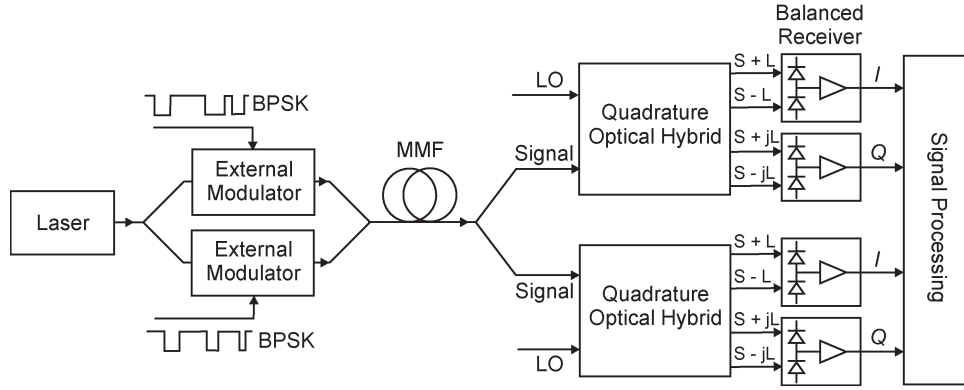$$

Fig. 2.   Block diagram of COMIMO showing two independently modulated carriers and two receivers. Coupling diversity is not shown for simplicity.
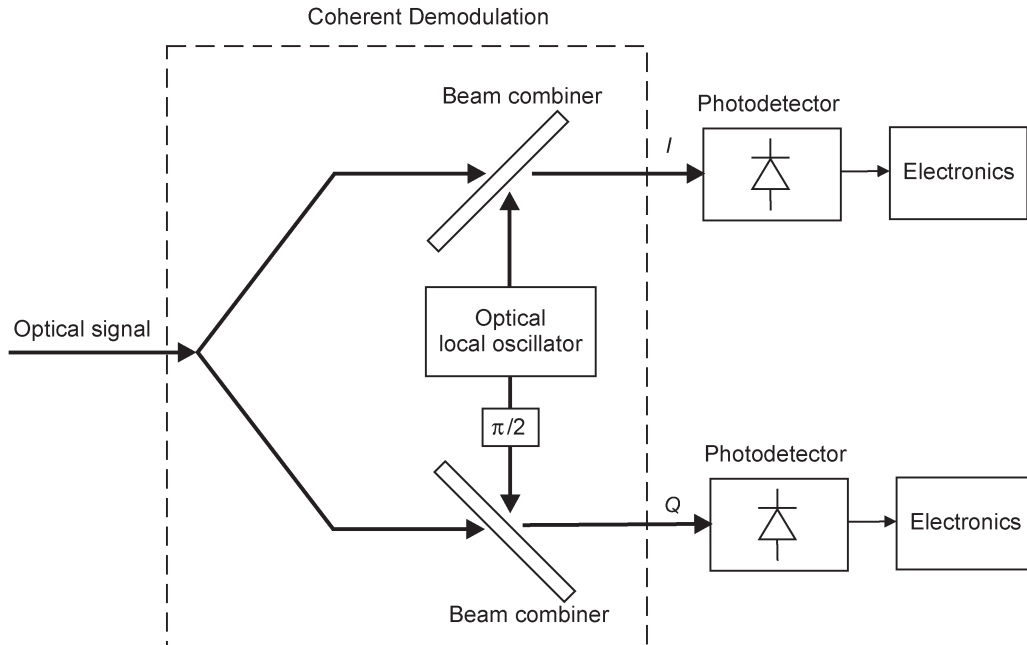

Fig. 3.   Details of coherent demodulation to produce I and Q baseband signals for MIMO decoding/equalization.

where each $\tilde{s}$ is now the following matrix of received data

$$\begin{pmatrix} y_1(1) & \dots & y_M(1) & y_1(0) & \dots & y_M(1-Q) \\ y_1(2) & \dots & y_M(2) & y_1(1) & \dots & y_M(2-Q) \\ \vdots & \ddots & \vdots & \vdots & \ddots & \vdots \\ y_1(Q) & \dots & y_M(Q) & y_1(Q-1) & \dots & y_M(0) \\ \vdots & \ddots & \vdots & \vdots & \ddots & \vdots \\ y_1(l) & \dots & y_M(l) & y_1(l-1) & \dots & y_M(l-Q) \end{pmatrix}$$

and $\mathbf{0}$ is the $l \times MQ$ zero matrix. In other words, $\tilde{\mathbf{S}}$ is a block diagonal matrix of *block size* $N \times N$, where each nonzero block is the $l \times MQ$ matrix $\tilde{s}$ that represents the received data. Both (4) and (7) can be solved recursively using adaptive filtering algorithms such as LMS or RLS for a real-time implementation [20].

III. IMPLEMENTATION

We have built a proof-of-concept 2×2 coherent optical MIMO system as shown in Figs. 2 and 3. A 1545-nm laser

output is split into two parallel arms which are binary phase-shift keying (BPSK)-modulated using standard $\mathrm{LiNbO_3}$ modulators. An MMF directional coupler is used to combine two input arms into 62.5-μm MMF before another coupler is used to separate and direct two different outputs to two detectors. Each input is coupled to the MMF with a slightly different modal power distribution. The sequence of MMF launching, connection, combining, and splitting creates a natural tendency for each detector to receive power from both transmitters via a different distribution of modes.

The local laser oscillator for coherent demodulation is derived from the original narrow linewidth laser source. This simplifies the experiment and is sufficient for a conceptual demonstration of COMIMO by ensuring phase and frequency locking. A more practical approach would be to use an optical phase-locked loop (PLL), a variety of which have been demonstrated elsewhere [23]. The transmitted signal S and the local oscillator L are directed into the commercial lithium niobate quadrature optical hybrid which gives two pairs of outputs 1) $S + L$, 2) $S - L$, and 3) $S + jL$, 4) $S - jL$. 1) and 2), and 3) and 4) are collected by two balanced detectors. This provides
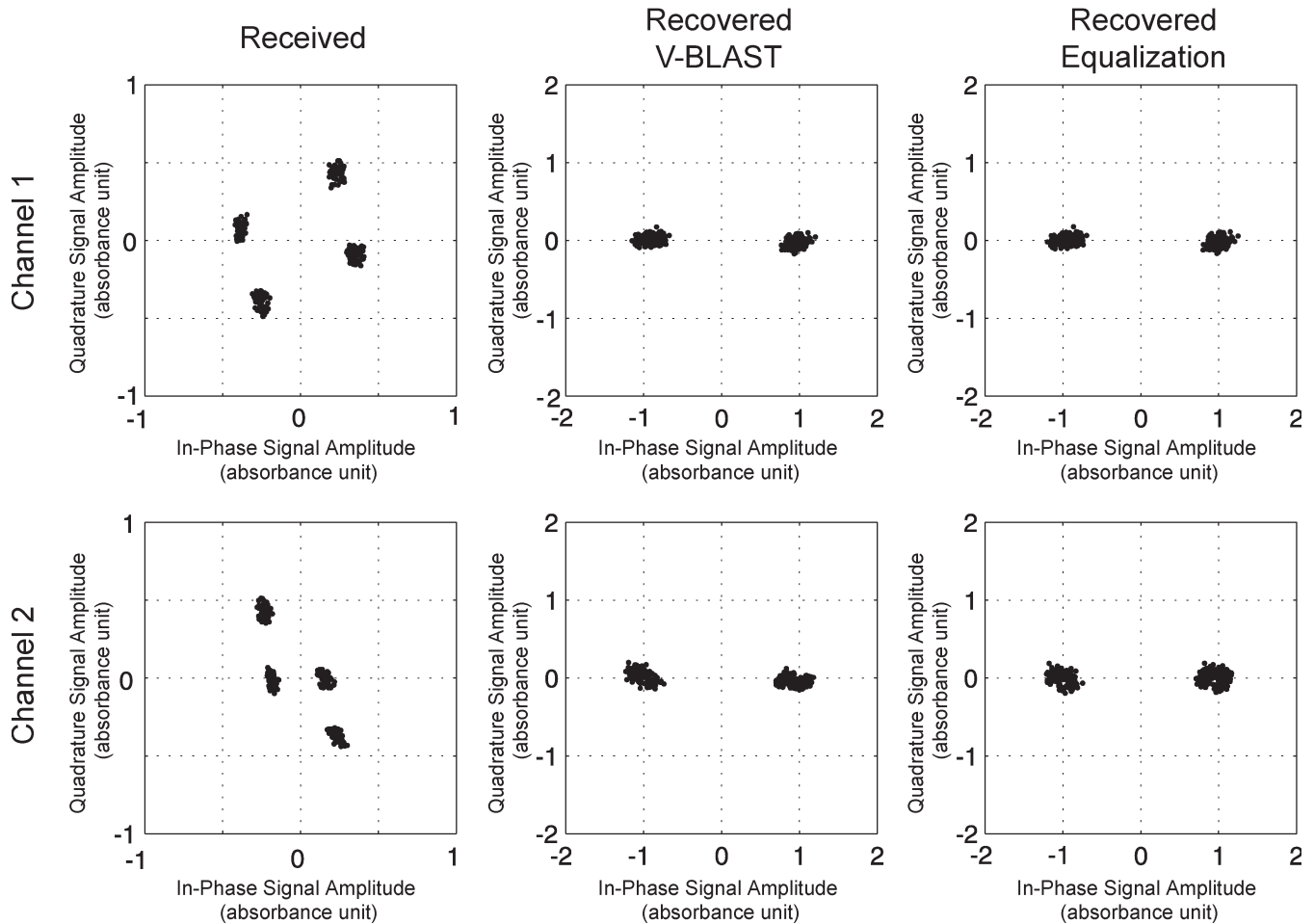
Fig. 4.   Constellation diagrams showing received data from a narrow-band channel and symbol recovery without equalization and with equalization.

the full signal–space information of the baseband signal, i.e., both I and Q components. These are digitized and applied to the signal processing algorithm (done offline in the computer program) for MIMO symbol recovery. MIMO signal processing consists of two steps: 1) estimating the channel matrix **H** using a sequence of training symbols and 2) using the channel estimate to recover the transmitted symbols.

Fig. 4(a) shows the complete signal–space constellations for two receivers in a 2×2 COMIMO system where 100 m of 62.5-μm MMF is used, with a data rate of 800 Mb/s. The four clusters of points in the constellation diagram, corresponding to transmitted symbol pairs {1,1}, {1,−1}, {−1,1}, and {−1, −1}, manifest the modal-coupling diversity at the input end of the fiber. If sufficient diversity does not exist, the symbol pairs {−1,1} and {−1, −1} will overlap in the constellation and will not be distinguishable. The fact that they are distinguishable in Fig. 4(a) is the indication that sufficient transmitter diversity is achieved. Furthermore, modal-coupling diversity present at the output end of the fiber causes the constellations for the two receivers to be different. This clearly demonstrates the required Tx/Rx diversity in the system for MIMO operation. After applying two types of MIMO signal processing algorithms separately to the received data set, one without and one with equalization, the data are restored in a BPSK signal–space as shown, respectively, in Fig. 4(b) and (c). The constellations

that result from both of these algorithms are very similar due to the lack of ISI, and both show good localization of points and hence increased likelihood of a correct decision. Specifically, the 256-bit transmitted data streams in both channels are correctly recovered, with no errors. For the present experiment, we have determined that ten training symbols are sufficient to obtain an accurate channel estimate and to recover error-free data. The condition number of the estimated channel matrix is 1.8 in this example. Such a well-conditioned channel matrix validates the existence of sufficient diversity and the accuracy of symbol recovery.

To demonstrate MIMO equalization, we performed a second experiment where we purposely exceeded the bandwidth–length product of the MMF, using a link of 2.8 km and again a data rate of 800 Mb/s. Fig. 5(a) clearly shows the impact of ISI on the received constellation through greater diffusion of the received points compared with the narrow-band case shown in Fig. 4(a).

A training sequence consisting of 50 of the 256 total transmitted symbols was used for channel estimation to apply the V-BLAST algorithm, resulting in the recovered constellation shown in Fig. 5(b). Note the residual diffusion of points due to ISI from the wide-band MIMO channel. Fig. 5(c) shows the recovered data using adaptive MIMO equalization, where for fair comparison to V-BLAST, 50 symbols were used to train the
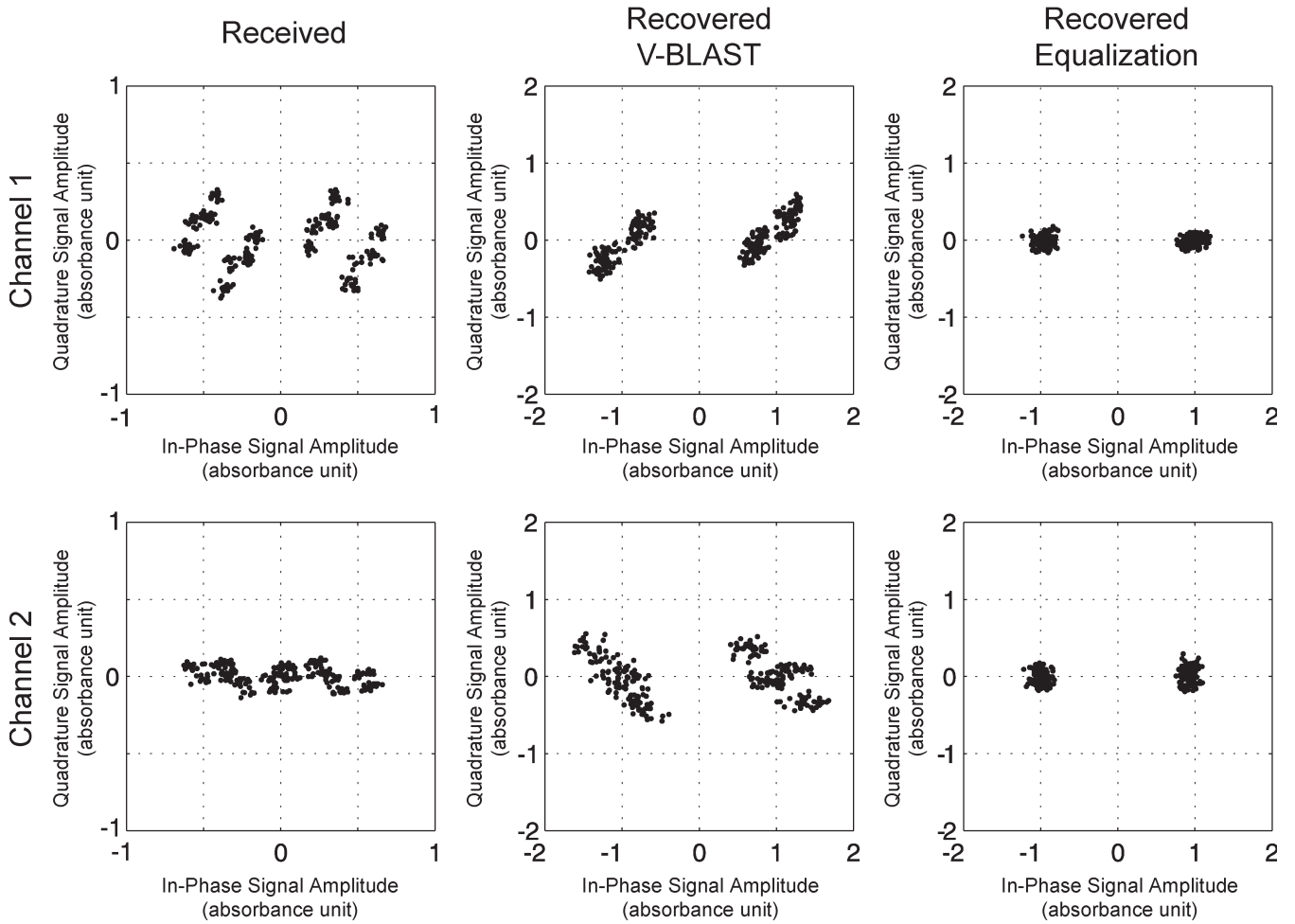
Fig. 5.   Constellation diagrams showing received data from a wide-band channel (with ISI) and symbol recovery without equalization and with equalization.
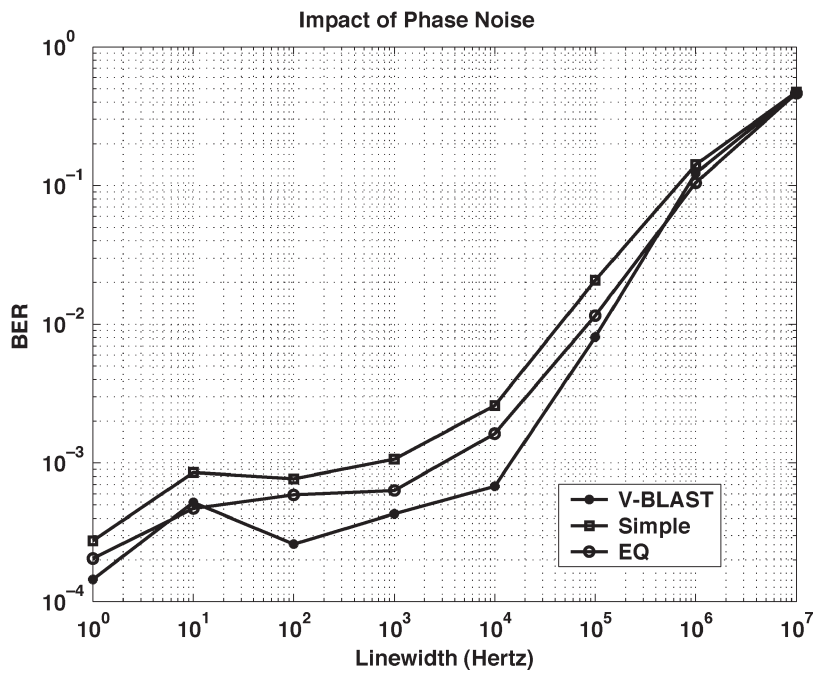

Fig. 6.   BER performance versus linewidth using various algorithms.

equalizers. By actually compensating for ISI, the equalization algorithm is better at localizing the cluster of received symbols and hence increasing the likelihood of a correct decision by a BPSK quantizer.

COMIMO is a coherent optical scheme and an important specification is the local oscillator (LO) laser phase noise that is modeled as an independent multiplicative noise source for each of the received signals, which in turn have unity magnitude and Gaussian-distributed random phase with a variance proportional to the LO laser linewidth. The distortion due to LO phase noise will then appear as a random rotation of points in the received constellation. The variance of phase noise (modeled as having a Gaussian distribution) is related to laser linewidth [24] simply as

$$\langle \sigma_\phi^2 \rangle = 2\pi \left(\frac{\Delta \nu}{f_{\mathrm{BW}}} \right) \tag{10}$$

where $\Delta \nu$ is the laser linewidth and f_{BW} is an optical PLL loop-bandwidth. This model leads to the usual Lorentzian spectral power density for a laser. Phase noise will affect the received signal as a multiplicative distortion of unity magnitude and random phase. For example, the narrow-band model with phase noise can be written as $y(t) = e^{j\phi(t)} h s(t - \tau_{\mathrm{g}}) + v(t)$, where $\phi(t)$ is the Gaussian-distributed random phase at the sampling time instant t. The impact of phase noise on uncoded bit error rate (BER; no error-correction coding) for a 2×2 system was studied with Monte Carlo simulations, using 1000 realizations of randomly generated channel matrices (narrow-band Rayleigh fading) for various values of laser linewidth. For each channel realization, 100 randomly generated BPSK symbols were sent from each transmitter. In addition, a 30-dB SNR without phase noise was assumed at each receiver to set the noise power for the additive white Gaussian noise (AWGN) source. The variance of the random-phase variable is set under the assumption of a 10-MHz optical PLL bandwidth, which is certainly realistic [23]. The uncoded BER performance under these conditions is shown in Fig. 6 and shows the departure from an AWGN-dominated system to a phase-noise-dominated system at a laser linewidth beyond 10 KHz (or a phase variance greater than $2\pi \times 10^{-3}$). Such a requirement for laser linewidth is very reasonable for coherent optical systems in general and is thus a further validation of the practical feasibility of COMIMO. Algorithms to specifically correct for residual phase noise (in addition to an optical-PLL) are under investigation. The absolute values of the BER scale in Fig. 6 are low due to an artificially high background AWGN SNR (30 dB). Using more reasonable values for AWGN SNR (40–50 dB) would require a tremendous increase in simulation time to capture errors. Since we are only trying to ascertain the shape of the BER curve versus laser linewidth, vertical shifts of the graph are not important at this stage.

IV. CONCLUSION

In this paper, we have described and demonstrated a coherent optical MIMO (COMIMO) system. Theoretical foundation was provided followed by experimental demonstration of a link with and without significant intersymbol interference (ISI). A coherent implementation has the advantage of an optical carrier whose frequency is large enough to tolerate small phase-delay spreads and ensure the necessary random uniform phase distribution of multipaths needed for diversity. Furthermore, unlike previous optical multiple-input multiple-output (MIMO) efforts, this system does not require an radio frequency (RF) subcarrier and is thus not limited in modulation bandwidth and by the associated hardware. MIMO Equalization can be used to combat ISI in wide-band systems where the group-delay spread is comparable to the symbol period.

REFERENCES

[1] D. Gesbert, S. Mansoor, S. Da-shan, P. J. Smith, and A. Naguib, "From theory to practice: An overview of MIMO space-time coded wireless systems," *IEEE J. Sel. Areas Commun.*, vol. 21, no. 3, pp. 281–302, Apr. 2003.

[2] L. Raddatz, I. H. White, D. G. Cunningham, and M. C. Norwell, "Influence of restricted mode excitation on bandwidth of multimode fiber links," *IEEE Photon. Technol. Lett.*, vol. 10, no. 4, pp. 534–536, Apr. 1998.

[3] ——, "An experimental and theoretical study of the offset launch technique for the enhancement of the bandwidth of multimode fiber links," *J. Lightw. Technol.*, vol. 16, no. 3, pp. 324–331, Mar. 1998.

[4] L. Raddatz, I. H. White, D. G. Cunningham, M. C. Nowell, M. R. T. Tan, and S.-Y. Wang, "A fiber-optic m-ary modulation scheme using multiple light sources," presented at the Optical Fiber Conf., Dallas, TX, 1997, Paper WL36.

[5] X. Zhao and F. S. Choa, "Demonstration of 10-Gb/s transmissions over a 1.5-km-long multimode fiber using equalization techniques," *IEEE Photon. Technol. Lett.*, vol. 14, no. 8, pp. 1187–1189, Aug. 2002.

[6] S. E. Ralph, K. M. Patel, C. Argon, A. Polley, and S. W. McLaughlin, "Intelligent receivers for multimode fiber: Optical and electronic equalization of differential modal delay," in *15th Annu. Meeting Conf. Proc. IEEE Lasers Electro-Optics Society (LEOS)*, Glasgow, Scotland, Nov. 2002, vol. 1, pp. 295–296.

[7] L. Raddatz, D. Hardcare, I. H. White, R. V. Penty, D. G. Cunningham, M. R. T. Tan, and S.-Y. Wang, "High bandwidth data transmission in multimode fiber links using subcarrier multiplexing with VCSEL's," *Electron. Lett.*, vol. 34, no. 7, pp. 686–688, 1998.

[8] L. Raddatz and I. H. White, "Overcoming the modal bandwidth limitation of multimode fiber by using passband modulation," *IEEE Photon. Technol. Lett.*, vol. 11, no. 2, pp. 266–268, Feb. 1999.

[9] T. K. Woodward, S. Hunsche, A. J. Ritger, and J. B. Stark, "1.6 Gb/s BPSK transmission at 850 nm over 1 km of 62.5-μm-core multimode fiber using a single 2.5-GHz subcarrier," *IEEE Photon. Technol. Lett.*, vol. 11, no. 3, pp. 382–384, Mar. 1999.

[10] E. J. Tyler, M. Webster, R. V. Penty, and I. H. White, "Penalty free subcarrier modulated multimode fiber links for datacomm applications beyond the bandwidth limit," *IEEE Photon. Technol. Lett.*, vol. 14, no. 1, pp. 110–112, Jan. 2002.

[11] E. J. Tyler, M. Webster, R. V. Penty, I. H. White, S. Yu, and J. Rorison, "Subcarrier modulated transmission of 2.5 Gb/s over 300 m of 62.5 μm core diameter multimode fiber," *IEEE Photon. Technol. Lett.*, vol. 14, no. 12, pp. 1743–1745, Dec. 2002.

[12] L. B. Aronson, B. E. Lemnoff, L. A. Buckman, and D. W. Dolfi, "Low-cost multimode WDM for local area networks up to 10 Gb/s," *IEEE Photon. Technol. Lett.*, vol. 10, no. 10, pp. 1489–1491, Oct. 1998.

[13] L. A. Buckman, B. E. Lemoff, A. J. Schmit, R. P. Tella, and W. Gong, "Demonstration of a small form factor WWDM transceiver module for 10-Gb/s local area networks," *IEEE Photon. Technol. Lett.*, vol. 14, no. 5, pp. 702–704, May 2002.

[14] H. R. Stuart, "Dispersive multiplexing in multimode optical fiber," *Science*, vol. 289, no. 5477, pp. 281–283, Jul. 2000.

[15] C. J. Hsu, A. Shah, and B. Jalali, "Coherent optical multiple-input multiple-output communication," *IEICE Electron. Express*, vol. 1, no. 13, pp. 392–397, Oct. 2004.

[16] R. C. J. Hsu, A. Shah, and B. Jalali, "Coherent optical multiple-input multiple-output communication over multimode fiber," presented at the Microwave Photonics Conf. 2004, Ogunquit, ME, unpublished.

[17] P. Pepeljugoski, J. Schaub, J. Tierno, J. Kash, S. Gowda, B. Wilson, H. Wu, and A. Hajimiri "Improved performance of 10 Gb/s multimode fiber optic links using equalization," in *Proc. Optical Fiber Communication (OFC)*, Atlanta, GA, 2003, vol. 2, pp. 472–474.

[18] D. Lenz, B. Rankov, D. Erni, W. Bachtold, and A. Wittneben, "MIMO channel for modal multiplexing in highly overmoded optical waveguides," in *Int. Zurich Seminar on Communications*, Zurich, Switzerland, 2004, pp. 196–199.

[19] G. D. Durgin, *Space–Time Wireless Channels*. Upper Saddle River, NJ: Prentice-Hall, 2003.

[20] A. H. Sayed, *Fundamentals of Adaptive Filtering*. New York: Wiley, 2003.

[21] G. D. Golden, C. J. Foschini, R. A. Valenzuela, and P. W. Wolninasky, "Detection algorithm and initial laboratory results using V-BLAST space–time communication architecture," *Electron. Lett.*, vol. 35, no. 1, pp. 14–16, Jan. 1999.

[22] A. Maleki-Tehrani, B. Hassibi, and J. M. Cioffi, "Adaptive equalization of multiple-input multiple-output (MIMO) frequency selective channels," in *Conf. Rec. 33rd Asilomar Conf. Signals, Systems, and Computers*, Pacific Grove, CA, Oct. 1999, vol. 1, pp. 547–551.

[23] L. N. Langley, M. D. Elkin, C. Edge, M. J. Wale, U. Gliese, X. Huang, and A. J. Seeds, "Packaged semiconductor laser optical phase-locked loop (OPLL) for photonic generation, processing and transmission of microwave signals," *IEEE Trans. Microw. Theor. Tech.*, vol. 47, no. 7, pp. 1257–1264, Jul. 1999.

[24] K. Kikuchi, T. Okoshi, M. Nagamatsu, and N. Henmi, "Degradation of bit-error rate in coherent optical communications due to spectral spread of the transmitter and the local oscillator," *J. Lightw. Technol.*, vol. 2, no. 12, pp. 1024–1033, Dec. 1984.

Alireza Tarighat (S'00) received the B.Sc. degree in electrical engineering from Sharif University of Technology, Tehran, Iran, in 1998 and the M.Sc. degree in electrical engineering from the University of California, Los Angeles (UCLA), in 2001, with emphasis on integrated circuits and systems. Since April 2002, he has been working toward the Ph.D. degree in electrical engineering at UCLA.

He was, during the summer of 2000, with Broadcom, El Segundo, CA, where he worked on designing IEEE 802.11a transceivers. From 2001 to 2002, he was with Innovics Wireless, Los Angeles, CA, as a Senior Design Engineer working on application-specific integrated circuit implementation of antenna diversity and rake processing for 3G wide-band code-division multiple-access mobile terminals. His research focuses on signal processing techniques for communications, including multiple-input multiple-output (MIMO) orthogonal frequency-division multiplexing receiver design and multiuser MIMO communications.

Mr. Tarighat was the recipient of the Gold Medal of the National Physics Olympiad, Iran, 1994 and the Honorable Mention Diploma of the 25th International Physics Olympiad, Beijing, China, 1994.

Akhil R. Shah received the B.S. degree in physics and electrical engineering from the University of California, Irvine, in 2000 and the M.S. degree in electrical engineering from the University of California, Los Angeles (UCLA) in 2003. Currently, he is working toward the Ph.D. degree with the Department of Physics at UCLA.

He has worked in industry since 2000, characterizing and designing radio-frequency integrated circuits, and modeling novel photonic devices. His current research interests are quantum communication and mathematical physics.

Rick C. J. Hsu received the B.S. degree in physics and the M.S. degree in electrical engineering from the National Taiwan University, Taipei, Taiwan, R.O.C., in 1999 and 2001, respectively. Since 2003, he has been working toward the Ph.D. degree with the Department of Electrical Engineering at the University of California, Los Angeles (UCLA).

His current research interests are in fiber-optic communication systems and microwave photonics.

Ali H. Sayed (S'90–M'92–SM'99–F'01) received the Ph.D. degree in electrical engineering from Stanford University, Stanford, CA, in 1992.

He is currently Professor and Vice-Chair of Electrical Engineering at the University of California, Los Angeles (UCLA). He is also the Principal Investigator of the UCLA Adaptive Systems Laboratory www.ee.ucla.edu/asl). He has over 200 journal and conference publications, is the author of the textbook *Fundamentals of Adaptive Filtering* (New York: Wiley, 2003), and is coauthor of the research monograph *Indefinite Quadratic Estimation and Control* (Philadelphia, PA: SIAM, 1999) and of the graduate-level textbook *Linear Estimation* (Englewood Cliffs, NJ: Prentice-Hall, 2000). He is also co-editor of the volume *Fast Reliable Algorithms for Matrices With Structure* (Philadelphia, PA: SIAM, 1999). He is a member of the editorial boards of the *SIAM Journal on Matrix Analysis and Its Applications* and the *International Journal of Adaptive Control and Signal Processing* and has served as co-editor of special issues of the journal *Linear Algebra and Its Applications*. He has contributed several articles to engineering and mathematical encyclopedias and handbooks and has served on the program committees of several international meetings. He has also consulted with industry in the areas of adaptive filtering, adaptive equalization, and echo cancellation. His research interests span several areas, including adaptive and statistical signal processing, filtering and estimation theories, signal processing for communications, interplays between signal processing and control methodologies, system theory, and fast algorithms for large-scale problems.

Dr. Sayed is a recipient of the 1996 IEEE Donald G. Fink Award, a 2002 Best Paper Award from the IEEE Signal Processing Society in the area of Signal Processing Theory and Methods, and coauthor of two Best Student Paper awards at international meetings. He is also a recipient of the 2003 Kuwait Prize in Basic Sciences. He is a Member of the Technical Committees on Signal Processing Theory and Methods (SPTM) and on Signal Processing for Communications (SPCOM), both of the IEEE Signal Processing Society. He is a Member of the Editorial Board of the IEEE SIGNAL PROCESSING MAGAZINE. He has also served twice as Associate Editor of the IEEE TRANSACTIONS ON SIGNAL PROCESSING, of which he is now serving as Editor-in-Chief.

Bahram Jalali (S'86–M'89–SM'97–F'03) received the B.S. degree in physics from Florida State University, Tallahassee, in 1984 and the M.S. and Ph.D. degrees in applied physics from Columbia University, New York, in 1986, and 1989, respectively.

He was a Member of Technical Staff at the Physics Research Division of AT&T Bell Laboratories, Murray Hill, NJ, from 1988 to 1992, where he conducted research on ultrafast electronics and optoelectronics. He was responsible for the successful development and delivery of 10 Gb/s lightwave circuits to the U.S. Air Force in 1992. He is a Professor of Electrical Engineering, the Director of the DARPA Center for Optical A/D System Technology (COAST), and the Director of the Optoelectronic Circuits and System Laboratory at the University of California, Los Angeles (UCLA). Dr. Jalali has over 200 publications and holds six U.S. patents. While on leave from UCLA from 1999 to 2001, Dr. Jalali founded Cognet Microsystems, Los Angeles, CA, a fiber-optic-component company. He served as Cognet's CEO, President, and Chairman, from the company's inception through its acquisition by Intel Corporation in April 2001. From 2001 to 2003, he served as a Consultant in the Communication Group of Intel Corporation. Dr. Jalali serves on the Board of Trustees of the California Science Center. His current research interests are in microwave photonics, integrated optics, and fiber-optic ICs.

Dr. Jalali is the Chair of the Los Angeles Chapter of the IEEE Lasers and Electro Optics Society (LEOS). He was the General Chair for the IEEE International Conference on Microwave Photonics (MWP) in 2001 and its Steering Committee Chair from 2001 to the present. He is also a Member of the California Nano Systems Institute (CNSI). He received the BridgeGate 20 Award in recognition of his contributions to the economy of Southern California.